

Ionization–excitation of lithium by fast charged projectiles

L Nagy¹, F Járαι-Szabó¹ and S Fritzsche²

¹ Faculty of Physics, Babeş-Bolyai University, Str. Kogălniceanu, Nr. 1, 400084 Cluj-Napoca, Romania

² Institut für Physik, Universität Kassel, Heinrich-Plett-Str. 40, D-34132 Kassel, Germany

E-mail: lnagy@phys.ubbcluj.ro

Received 10 June 2004, in final form 7 December 2004

Published 24 January 2005

Online at stacks.iop.org/JPhysB/38/141

Abstract

Cross sections for the double K-shell vacancy production of lithium atoms in collision with fast charged projectiles are calculated. For these ionization–excitation processes, the relative importance of the different first- and second-order mechanisms and the dependence of the cross sections on the sign of projectile charge are investigated. Our studies confirm the strong influence of electron–electron correlations on the behaviour of the cross sections. The obtained results are in reasonable agreement with the data as observed in recent experiments.

1. Introduction

Electronic excitations of inner-shell electrons in atomic lithium are very good examples for the importance of electron correlations in atomic scattering and collisions. As shown previously for the excitation of a single K-shell electron [1], the observed cross sections can be reproduced by theory only if correlated wavefunctions are applied for both the initial bound state and the final scattering states of lithium.

The formation of K-shell vacancy states of lithium by fast charged projectiles has been studied experimentally by Tanis and co-workers [2, 3] during recent years. In the experiments, this process is observed by means of the Auger emission which follows the creation of a K-shell hole. The cross sections for different excited states could be resolved by analysing the Auger electron spectra. A similar (experimental) situation also occurs for simultaneous ionization and excitation of the two K-shell electrons which results in a hollow Li⁺ ion. In the Auger spectra, the decay of these hollow atoms is observed by the KLL satellite lines (these transitions being a satellite to the dominant ones with a single K-shell vacancy). For both excitation processes, the single K-shell excitation and the double K-shell vacancy formation of Li by fast electron impact, new experimental data have been published recently [4]. In practice, these inner-shell excitations can be explained only if the electron–electron

interactions are considered properly by going beyond any mean-field approximation. While, from the viewpoint of the experimentalists, the creation of the S states of Li^+ is caused by shake processes, the production of the P states is believed to follow dielectronic processes (sometimes also called TS1). To test this assumption, a detailed study has been carried out for the formation of hollow Li^+ ions by the impact of atomic lithium with charged particles.

In a previous study [1], the single K-shell excitation of Li has been described successfully by applying multiconfiguration Hartree–Fock (MCHF) wavefunctions for the initial and final states. In this investigation electron–electron correlations were included into the wavefunctions by making use of a proper superposition of configuration state functions, having the same overall symmetry. In the present work, we have now applied a very similar method for the double K-shell vacancy production. Our aim is to identify the main mechanisms which lead to the formation of the ‘hollow K-shell ions’ Li^+ as well as to analyse the cross sections in dependence on the velocity of the projectiles and their charge sign.

2. Theoretical assumptions

In the present computations, the semiclassical impact-parameter method is adopted for the collision of fast charged projectiles with neutral atoms, together with second-order perturbation theory. In this approximation, the projectile moves along a classical, straight-line trajectory which can be characterized by means of an impact parameter B . From a theoretical viewpoint, of course, this implies that only the electronic system needs to be described by a time-dependent Schrödinger equation, while the projectile follows classical laws throughout and only enters the theoretical treatment of the collisions due to its charge and velocity. Using second-order perturbation theory, then the first- and second-order transition amplitudes can be written as

$$a^{(1)} = -i \int_{-\infty}^{+\infty} dt \exp(i(E_f - E_i)t) \langle f | V(t) | i \rangle \quad (1)$$

$$a^{(2)} = - \sum_k \int_{-\infty}^{+\infty} dt \exp(i(E_f - E_k)t) \langle f | V(t) | k \rangle \int_{-\infty}^t dt' \exp(i(E_k - E_i)t') \langle k | V(t') | i \rangle, \quad (2)$$

where i , k and f represent the initial, intermediate and final electronic states of the collision system, respectively. Similarly, E_i , E_k and E_f are the energies of the corresponding (unperturbed) states of the system while $V(t)$ denotes the time-dependent interaction between the projectile and the electrons.

In most computations on ion–atom collision, the outcome of the calculations are known to be very sensitive to the treatment of electronic correlations. This has to be expected, in particular, for describing all ionization–excitation processes where the Lienard–Wiechert potential in the ion collision causes a simultaneous re-occupation of at least two electrons in lithium. A completely *correlated computation* of this process, however, goes much beyond what is feasible today by present-day computer. In order to incorporate at least the dominant parts of the electron correlations in the initial and final wavefunctions, the multiconfiguration Hartree–Fock method has been applied to generate the bound-state orbitals. Since, in this method, the wavefunctions are obtained self-consistently, this includes the relaxation of the bound-state density if both the K-shell electrons are removed from the neutral Li atom. For the construction of the final scattering states, however, the continuum orbitals have been generated in the mean field of the final ion, neglecting the interaction among the different continua. Thus, the continuum–continuum interaction is taken into account only partially, while the electron–electron correlations in the bound-state densities are well represented.

The bound-state wavefunctions have been generated by means of the GRASP92 [5] and RATIP [6] programs. In these programs, atomic state functions are taken as linear combinations of symmetry-adapted configuration states and are optimized on the basis of the Dirac–Coulomb Hamiltonian. Although, this is a relativistic approach for the generation of the wavefunctions, a set of (two-component) non-relativistic orbitals have been subtracted by using only the large components and by a proper re-normalization of these functions. For the p and d orbitals, in addition, the two radial functions for $j = l \pm 1/2$ have first been averaged, an approximation which seems well justified as these radial functions ‘overlap’ to better than 99% for neutral lithium. For the $1s^2 2s^2 S_{1/2}$ ground-state function, an expansion including single and double excitation into the $n = 2$ and $n = 3$ shells (i.e., into the active set $\{1s, 2s, 2p, 3s, 3p, 3d\}$) have been considered. For the excited states of Li^+ an active set of $\{2s, 2p, 3s, 3p\}$ orbitals has been taken into account. In this approximation, we obtained energies which agree within 0.02% with the experimental value for the ground state of Li, and within 1% with the excited states of the Li^+ (except for the $2p^2 \ ^1S$ state with a disagreement of 3%). In contrast to the traditional use of the symmetry-adapted wavefunctions, however, an expansion into (two- or three-electron) Slater determinants has first been carried out in order to apply our previously developed collision code [7]. For time-dependent perturbation calculations, the use of determinants has the advantage that no ‘re-coupling’ of the angular momenta is required in the evaluation of the transition amplitudes (1) and (2). To our knowledge, in fact, no implementation is available where symmetry-adapted wavefunctions are used in time-dependent computations.

In a determinants basis, the lithium ground state is given by

$$\begin{aligned} i &= \sum_i c_i \det |\phi_{a_i}(r_1)\phi_{b_i}(r_2)\phi_{e_i}(r_3)| \\ &= \frac{1}{\sqrt{3!}} \sum_i c_i \sum_P (-1)^P P \phi_{a_i}(r_1)\phi_{b_i}(r_2)\phi_{e_i}(r_3) \end{aligned} \quad (3)$$

with expansion coefficients c_i as obtained from the self-consistent wavefunctions [5] and their subsequent expansion into Slater determinants. Similarly, the final scattering states can be written as

$$\begin{aligned} f &= \sum_j d_j \det |\phi'_{a_j}(r_1)\phi'_{b_j}(r_2)\phi'_{\text{cont}}(k, r_3)| \\ &= \frac{1}{\sqrt{3!}} \sum_j d_j \sum_{P'} (-1)^{P'} P' \phi'_{a_j}(r_1)\phi'_{b_j}(r_2)\phi'_{\text{cont}}(k, r_3), \end{aligned} \quad (4)$$

having two bound electrons and one in the continuum. Here, ϕ and ϕ' refer to two different sets of spin orbitals for the initial and final states, respectively, and P and P' denote the permutation of the corresponding orbitals. The bound orbitals are labelled by a_i, b_i and e_i , while ϕ'_{cont} refers to some continuum orbital of the emitted electron and has been calculated in the mean field of the residual ion. As for the ground state, the coefficients d_j refer to the bound-state computations of the final ionic state.

In the second-order amplitude (2), moreover, the summation over the complete set of intermediate states is restricted to those determinants which differ from the initial- and final-state determinants by the replacement of just a single electron. Although, obviously, this approximation neglects the correlation in the intermediate states, such a computational scheme is known to be well justified for fast collisions [8].

Taking into account that the perturbation is a sum of three individual terms of the projectile–electron interaction

$$V(t) = \sum_{l=1}^3 V_l(t), \quad (5)$$

the first-order amplitude of the transition can be written as

$$a^{(1)} = -\frac{i}{3!} \sum_{l=1}^3 \sum_{i,j} \sum_{P,P'} c_i d_j^* (-1)^{P+P'} P P' \times \langle \phi'_{a_j} | \phi_{a_i} \rangle \langle \phi'_{b_j} | \phi_{b_i} \rangle \int_{-\infty}^{+\infty} dt \exp(i(E_f - E_i)t) \langle \phi'_{\text{cont}} | V_l(t) | \phi_{e_i} \rangle, \quad (6)$$

where the continuum orbital ϕ'_{cont} either appears in the transition matrix element or in one of the overlap integrals. Since, in the second-order amplitudes, the correlation effects are less important, only the leading term in the expansions (3) and (4) for the initial and final states, respectively, has been taken into account explicitly

$$a^{(2)} = -\frac{1}{3!} \sum_{l,l'=1}^3 \sum_{P,P'} (-1)^{P+P'} P P' \langle \phi'_a | \phi_a \rangle \int_{-\infty}^{+\infty} dt \exp(i(E_f - E_{k_1})t) \langle \phi'_b | V_{l'}(t) | \phi_b \rangle \times \int_{-\infty}^t dt' \exp(i(E_{k_1} - E_i)t') \langle \phi'_{\text{cont}} | V_l(t') | \phi_e \rangle. \quad (7)$$

In this expression, moreover, all terms which contain two interactions with the same electron are neglected because the second-order process of a single electron is usually insignificant for fast collisions. From the first- and second-order amplitudes, the differential cross sections relative to the ejected electron momentum \mathbf{p} are obtained by integrating the square of the total amplitude over all values of the impact parameter B ,

$$\frac{d\sigma}{d\mathbf{p}} = 2\pi \int B dB |a^{(1)} + a^{(2)}|^2. \quad (8)$$

While the first-order amplitude is proportional to Z_p , the charge of the projectile, and the second-order amplitude proportional to Z_p^2 , now an interference term occurs in the total cross sections which is proportional to the third power of the charge, Z_p^3 . It is this term which is eventually responsible for the sign dependence of the cross sections on the projectile charge [9].

In order to obtain cross sections for the production of different excited states of Li^+ we integrate the differential cross section above over the angles and magnitude of the ejected electron momentum. Integration over the magnitude of the momentum has been done numerically using the positive half of a 16-point Gauss–Hermite formula, with the highest value of the momentum 5 au. The convergence of the integration has been checked by doubling the number of points and extending the highest momentum value, and errors have been kept below 2%.

3. Results and discussion

The correlated motion of the bound electrons gives rise to quite sizable wavefunction expansions for the initial and final states. Allowing single and double excitations into all shells up to $n = 3$, there are 646 determinants in the representation of the $1s^2 2s$ ground state

Table 1. Calculated cross sections (expressed in 10^{-20} cm²) for the production of different hollow Li⁺ states from the ground state of the lithium induced by 95 MeV u⁻¹ Ar¹⁸⁺ projectiles in comparison with experimental data [3]. The contributions of the first- and second-order mechanisms are listed separately.

State	First order	Second order	Theory	Experiment
2s ² ¹ S	3.56	0.422	3.99	3.6
2p ² ¹ S	2.67	0.0169	2.74	1.5
2s2p ³ P	8.62	2.07	10.7	9.3
2s2p ¹ P	2.02	0.689	2.68	4.6
2s3s ³ S	4.57	0.241	4.81	4.5
2s3s ¹ S	0.495	0.178	0.668	–

and 46 for the $2lnl'$ final excited states. To understand the double K-shell vacancy production, let us begin with fast ion collisions. Table 1 presents the results for 95 MeV u⁻¹ Ar¹⁸⁺ projectiles in comparison with the experimental data [3]. In order to display the importance of the first- and second-order mechanisms, their individual contributions to the cross sections are listed separately. As expected for $Z/v = 0.3$, with Z being the charge and v the velocity of the projectiles, the second-order contributions appear to be negligible for the production of most autoionizing states of Li⁺. The second-order term becomes significant only in the case of the P states which, in the language of single-particle excitations, are produced by two successive dipole transitions.

Some comments are in order here for the fact that the cross section for the 2s3s ³S state is larger than those for 2s² ¹S. This behaviour was first observed by Tanis *et al* [3, 4] and has been explained by the importance of the exchange-shake mechanism, i.e., by means of the successive $1s \rightarrow 2s$ and $2s \rightarrow 3s$ transitions in the target. Our calculations partially confirm this explanation in that the 2s3s ³S state is mainly produced by the projectile–electron interaction to ionize one of the K-shell electrons, together with the rearrangement of the remaining electrons in the ions. In our computations, the probability for a certain rearrangement is obtained by the overlap integral between the final and initial multiconfiguration two-electron wavefunctions. In order to identify the *direct* ($1s \rightarrow 3s$) and the *exchange* ($1s \rightarrow 2s$ ‘plus’ $2s \rightarrow 3s$) mechanisms, we have set to 0 all other shake possibilities. With this computational procedure, we then obtain cross sections of 2.25×10^{-20} cm² for the direct mechanism and of 4.35×10^{-20} cm² for the exchange mechanism. The interference between these two mechanisms, together with amplitudes as obtained from admixtures of further determinants, leads to a total first-order contribution of about 4.57×10^{-20} cm².

Further calculations have been performed for the case of electron and proton projectiles with quite different energies. The resulting cross sections for electron projectiles are displayed in table 2 in which the shake-up and shake-off processes are listed separately and together with the first- and second-order cross sections. Here, shake-off means the process of exciting one of the electrons followed by its ejection due to the rearrangement of the electrons, while shake-up denotes the ionization as caused by the projectile and followed by a later excitation through the rearrangement of electrons. The results are also compared with experimental data available [4, 10]. The private communication [10] refers to absolute cross sections, for several impact energies, not published in [4]. The cross sections for proton projectiles are not listed because the differences between results for electron and proton projectiles are less than 2.5% for all final states in the considered projectile velocity range. In the case of triplet final states higher cross sections are obtained for electron projectiles, while for singlet states cross sections for proton projectiles are slightly higher.

Table 2. Absolute cross sections for the formation of different double K-shell vacancy states (in 10^{-21} cm²) by different ionization–excitation processes, and compared with experiments [10]. Theoretical cross sections are shown separately for different processes (shake-up and shake-off, giving together the first-order contribution, the second-order contribution and the total). Calculations have been made for electron projectiles at three different energies (in keV).

State	Projectile energy	Shake off	Shake up	First order	Second order	Total	Experiment [10]
2s ² 1S	0.5	0.326	2.95	3.29	0.343	3.6	3.8
	1.5	0.14	1.53	1.69	0.049	1.73	1.9
	5	0.047	0.634	0.71	0.005	0.717	0.64
2p ² 1S	0.5	0.166	2.12	2.13	0.0009	2.12	2.2
	1.5	0.102	1.34	1.33	0.0004	1.32	0.44
	5	0.06	0.586	0.593	0.0001	0.59	0.15
2s3s 3S	0.5	0.828	4.81	5.64	0.182	5.83	4.7
	1.5	0.402	2.44	2.74	0.0273	2.77	2.1
	5	0.151	0.994	1.06	0.0027	1.06	0.85
2s3s 1S	0.5	0.0086	0.287	0.303	0.121	0.42	0.4
	1.5	0.0069	0.249	0.258	0.0182	0.277	0.2
	5	0.0043	0.113	0.118	0.0018	0.12	0.05
2s2p 3P	0.5	1.6	0.564	2.31	0.902	3.22	11.1
	1.5	1.4	0.387	1.86	0.134	1.99	2.9
	5	0.9	0.186	1.12	0.015	1.14	0.88
2s2p 1P	0.5	0.654	0.213	0.939	0.298	1.22	6.7
	1.5	0.313	0.147	0.5	0.0447	0.543	2.2
	5	0.134	0.0713	0.225	0.005	0.23	0.7
(2, 3sp) 3P	0.5	0.811	0.377	1.28	1.21	2.49	6.2
	1.5	0.577	0.264	0.882	0.185	1.06	2.16
	5	0.565	0.128	0.706	0.0212	0.726	0.58
(2, 3sp) 1P	0.5	0.284	0.102	0.383	0.405	0.789	2.15
	1.5	0.304	0.0727	0.363	0.0618	0.43	0.84
	5	0.365	0.0356	0.366	0.0071	0.375	0.23

As seen from table 2, different processes are responsible for the creation of the states within the impact-parameter model from above. The four ^{1,3}S states, for instance, are mainly formed by first-order shake-up processes, while the second-order processes are found to be negligible, at least for small ratios of Z/v . For the P states, in contrast, a *pure* shake-up process (that is the ionization of an electron by the projectile and the excitation of another electron to a P state owing to the rearrangement of the bound electrons) is not possible within a single-configuration approximation. This process becomes possible only if configuration interactions are taken into account which leads to spp admixtures to the initial-state wavefunctions. With these admixtures, a generalized shake process to P states is allowed after one of the K-shell electrons is ejected. Similarly, configuration interactions in the final state may also contribute to the production of P states.

The main contributions to the P state production arises, however, from the generalized shake-off, i.e., the excitation of one electron to a p orbital while the other electron is ejected due to the rearrangement of the electron density. For fully correlated wavefunctions of the initial and final states, these two mechanisms also include the dielectronic process as mentioned

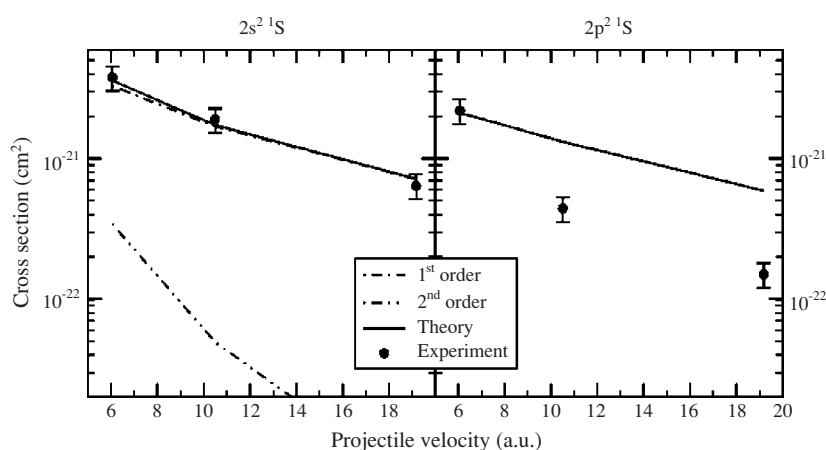


Figure 1. Calculated electron-impact ionization–excitation cross sections for $2s^2\ ^1S$ and $2p^2\ ^1S$ final states as a function of projectile velocity compared with experimental data [10].

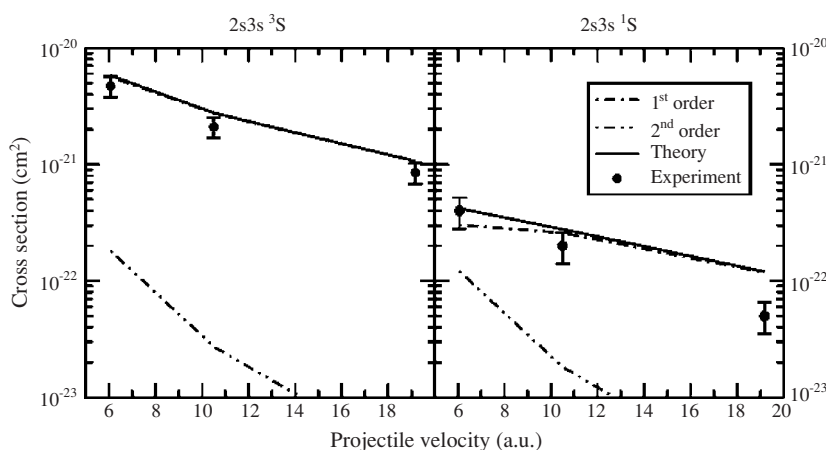


Figure 2. Same as figure 1 but for $2s3s\ ^3S$ and $2s3s\ ^1S$ final states.

by Tanis *et al* [3] and Rangama *et al* [4]. Since our final-state wavefunction are not much correlated, in particular if the interaction with the ejected electron is concerned, only parts of this dielectronic mechanism are included in the computations.

Comparing the results for the first- and second-order processes in table 2, we therefore conclude that second-order processes are negligible for high projectile energies and that they are of only minor importance at low energies. In figures 1–4, the dependence of the cross sections in the velocity of the projectiles is shown. They are displayed separately for the various final states of the ionization–excitation and are compared with existing experimental data [10, 4]. For each final state in figures 1–4, the contributions from the first- and second-order mechanisms as well as the total cross sections are shown explicitly.

Figure 1 shows theoretical cross sections for the ionization–excitation of the two K-shell electrons in lithium into the final $2s^2\ ^1S$ and $2p^2\ ^1S$ levels. For these levels, clearly, the first-order mechanisms are the dominant ones. For the formation of the $2s^2\ ^1S$ final state, in particular, the second-order effects become visible at low energies of the projectiles but are completely negligible at all high energies. As seen from the left panel of this figure, the

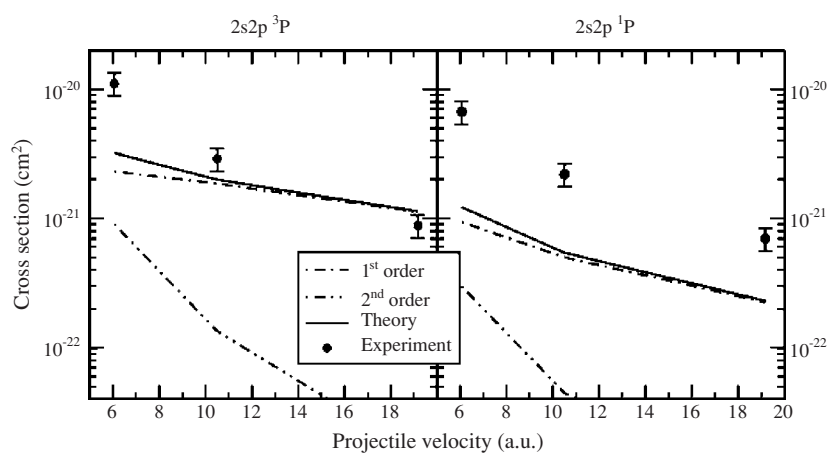


Figure 3. Same as figure 1 but for $2s2p\ ^3P$ and $2s2p\ ^1P$ final states.

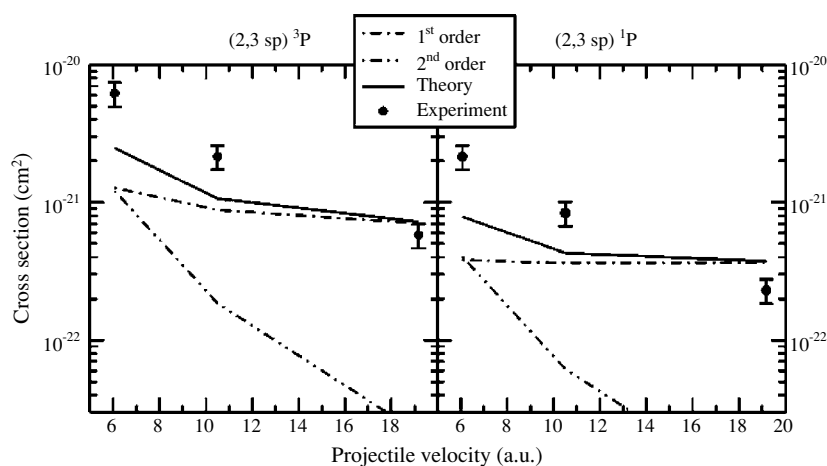


Figure 4. Same as figure 1 but for $(2, 3sp)\ ^3P$ and $(2, 3sp)\ ^1P$ final states.

obtained results are in very good agreement with experiment [10]. For the $2p^2\ ^1S$ final state, moreover, the first-order term dominates the cross sections within the entire range of projectile velocities. This can be understood from the fact that no direct second-order process contributes to the $2p^2\ ^1S$ level but that it is mainly formed by two $1s \rightarrow 2p$ processes and followed by a $1s \rightarrow$ continuum-shake mechanism. In contrast to the experiment, the theoretical data show a much slower decrease of the cross sections as a function of the projectile velocity. The disagreement between the theory and experiment at high velocities is mainly due to the incomplete description of the final-state correlations. Because in the excitation of the $2p^2\ ^1S$ state correlation plays a more important role than for the production of the $2s^2\ ^1S$ state (which is possible also by simple shake), results for the latter are obtained closer to the experimental data.

The calculated cross sections for the $2s3s\ ^3S$ and $2s3s\ ^1S$ final states are presented in figure 2. For the triplet states, the first-order process is again by far the dominant contribution and is in good agreement with experiment. For the $2s3s\ ^1S$ singlet state, the influence of the second-order mechanisms is seen at low electron velocities and leads to an overall decrease

of the cross sections. These cross sections are however too large for high electron energies when compared with experiment. Figure 3 displays the analogous cross sections for the $2s2p\ ^3P$ and $2s2p\ ^1P$ levels. For these final states, the second-order mechanisms play a much more pronounced role than for the S states. Here, the theoretical results show only a qualitative agreement with experiment, again because the correlation in the final state was not described completely. The approximations in the computations of the second-order amplitude, the neglect of the correlation in this case and the missing terms in the representation of the intermediate states may also contribute to the discrepancy.

The dependence of the cross sections for the $(2, 3sp)\ ^3P$ and $(2, 3sp)\ ^1P$ states on the velocity of the projectiles is shown in figure 4. These final states are formed by the $2s3p$ and $3s2p$ states which are energetically very close to each other and cannot be resolved experimentally. For this reason, we have summed over the cross sections for the individual levels. With this summation, our results in figure 4 shows reasonable agreement with the data from experiment.

Figures 1–4 show that the theoretical results are in reasonable agreement with experiment for electron projectiles. Moreover, only a minor change occurs in the cross sections if the charge of the projectile changes its sign. Therefore, there is no need to draw the cross sections also for proton impact in these figures.

4. Conclusions

The formation of double K-shell vacancy configurations in atomic lithium by $95\text{ MeV u}^{-1}\text{ Ar}^{18+}$ ion impact and by 0.5 keV , 1.5 keV and 5 keV electron projectiles has been investigated theoretically using the impact-parameter approximation and second-order perturbation theory. While in the first-order calculations, the configuration interactions between the bound electrons were taken into account, the second-order computations are carried out in single configuration by just including the leading term in the determinant expansion of the wavefunctions. In most cases, the obtained cross sections for the formation of an empty K-shell show good agreement with the experimental data available. The discrepancies between theory and experiment for the production of some final states may be explained by the incomplete description of the electron correlations in the final state. Although our method does not lead to perfect results in all cases, these are the first complex calculations which describe the double K-shell vacancy production in lithium. It is found that for the projectile velocities down to about 5 au (for a projectile charge equal to unity), the ionization–excitation cross sections do not depend significantly on the charge sign of the projectile, a fact which can be explained by the small influence of the second-order processes. For the formation of S states with a double K-shell vacancy, the total cross section is dominated by the first-order shake-up processes. For the P states, in contrast, both the generalized shake-up and shake-off processes give rise to significant contributions. In this generalized shake process, there are also included final-state correlations which were described by Tanis *et al* [3] and Rangama *et al* [4] as dielectronic processes.

Acknowledgments

Support from the Bergen Computational Physics Laboratory in the framework of the European Community—Access to Research Infrastructure Programme and the Research Institute of Sapientia Foundation is acknowledged.

References

- [1] Nagy L and Fritzsche S 2000 *J. Phys. B: At. Mol. Opt. Phys.* **33** L495
- [2] Tanis J A *et al* 1999 *Phys. Rev. Lett.* **83** 1131
- [3] Tanis J A *et al* 2000 *Phys. Rev. A* **62** 032715
- [4] Rangama J, Hennecart D, Stolterfoht N, Tanis J A, Sulik B, Frémont F, Husson X and Chesnel J-Y 2003 *Phys. Rev. A* **68** 040701
- [5] Parpia F A, Froese Fischer C and Grant I P 1996 *Comput. Phys. Commun.* **94** 249
- [6] Fritzsche S 2001 *J. Electron Spectrosc. Relat. Phenom.* **114–116** 1155
- [7] Nagy L 2000 *Nucl. Instrum. Methods B* **154** 123
- [8] Bronk T, Reading J F and Ford A L 1998 *J. Phys. B: At. Mol. Opt. Phys.* **31** 2477
- [9] Nagy L, McGuire J H, Végh L, Sulik B and Stolterfoht N 1997 *J. Phys. B: At. Mol. Opt. Phys.* **30** 1239
- [10] Chesnel J-Y 2002 Private communication